The NO Dimer, ^{14}N and ^{15}N Isotopomers Isolated in Argon Matrix: A Near-, Mid-, and Far-Infrared Study

Lahouari Krim* and Nelly Lacome

Laboratoire de Spectrochimie Moléculaire, URA CNRS 508, Université Pierre et Marie Curie, Bat F74, Case 49, 4 Place Jussieu, 75252 Paris, Cedex 05, France

Received: October 13, 1997; In Final Form: January 21, 1998

A near- and far-infrared study of $^{14}NO-^{14}NO$ and its isotopomers, $^{14}NO-^{15}NO$ and $^{15}NO-^{15}NO$, isolated in argon matrix has been carried out. Infrared active fundamental vibrational modes, ν_1, ν_2, ν_3, ν_5, and ν_6, for each species of the dimer have been observed, as well as overtone bands $2\nu_1$, $2\nu_5$ and combination bands $\nu_1 + \nu_5$, $\nu_1 + \nu_6$, $\nu_5 + \nu_6$, and $\nu_4 + \nu_5$. Frequency of the nonactive ν_4 mode was also retrieved from combination bands. From the knowledge of the 18 available frequencies of the three isotopic species, force constants for the *cis*-ON−NO have been calculated. The force constants characterizing the N−N stretching mode and the ONN bending mode are found to be 0.39 mdyn/Å and 0.42 mdyn Å/rad^2, respectively. The potential energy distribution calculated for each vibration showed that the ν_2 and ν_3 modes are strongly coupled and that there is no pure N−N stretching mode. In the same way, the ν_1 mode could be considered as a pure NO stretching mode while the ν_5 one is coupled to the ONN bending.

1. Introduction

Spectroscopy of the NO dimer has been the subject of a large number of studies in the gas phase[1] as well as in molecular beams[2] or under matrix isolation conditions.[3−5] The aim of these studies was the evaluation of the binding energy, the determination of the frequencies of intermolecular vibrational modes, and also the characterization of the possible geometries of the dimer. Several shapes of the NO dimer have already been recognized, all of them corresponding to a planar configuration: *cis*-ONNO, *trans*-ONNO, *cis*-ONON, and *trans*-ONON. It is now well established that the most stable geometry corresponds to the cis form ON−NO with a N−N bond. The frequencies of the different vibrational modes of the *cis*-$(^{14}N^{16}O)_2$ found in the literature[6] are listed in Table 1.

As shown from this table, strong scatter of values is observed for the results derived from infrared and Raman spectra.[7,8] While for high-frequency modes, corresponding to the N═O symmetric stretch ν_1 and the N═O asymmetric stretch ν_5, the results appear to be in reasonable agreement,[9−17] on the contrary, low-frequency modes corresponding to bendings or torsion exhibit large discrepancies between authors. For example, for the frequency of the ν_6 N−N═O asymmetric bending, the observed values range from 167 up to 768 cm^{-1}.[6,18,19]

Investigation of isotopomers of $(NO)_2$ were reported as early as 1969 by Guillory and Hunter[20] and 1976 by Durig and Griffin.[7] Raman spectra of *cis*-nitric oxide dimer, $(^{14}N^{16}O)_2$, and its isotopomers $^{16}O^{15}N^{15}N^{16}O$ and $^{18}O^{14}N^{14}N^{18}O$ have been extensively studied by Nour et al.[8] They observed for the fundamental modes ν_1 through ν_6 of $(^{14}N^{16}O)_2$ frequencies located at 1866, 266, 187, 97, 1762, and 214 cm^{-1}, respectively.

The present work is devoted to the high-resolution IR spectroscopy of $^{14}NO^{-14}NO$, and its isotopically substituted forms $^{14}NO-^{15}NO$ and $^{15}NO-^{15}NO$, isolated in argon matrixes. A subsequent study will report the results observed for $(NO)_2$ trapped in nitrogen matrixes.[21] The spectral domain investigated lies from 6000 down to 100 cm^{-1}. Therefore, several vibrational frequencies could be observed for each one of the aforementioned isotopic species. In particular, bands from, ν_2 N−N stretch as well as ν_3 N−N═O symmetric and ν_6 asymmetric bends were observed in the far-IR region. Furthermore, overtone and combination bands of N═O symmetric ν_1 and asymmetric ν_5 stretches such as $\nu_1 + \nu_5$, 2 ν_1, and 2 ν_5 could be also recorded in the mid- and near-IR range. Isotopic substitution was accordingly used for clarifying the assignments of all vibrational modes of the dimer.

TABLE 1: Vibrational Frequencies of *cis*-ONNO

mode	approximate type	activity	frequency (cm^{-1})			
ν_1	NO symmemtric stretch	infrared, Raman	1863	1866	1866	1863.6
ν_2	N−N stretch	infrared, Raman	266	176	266	
ν_3	N−N═O symmetric bend	infrared, Raman	182	264	187	
ν_4	torsion	Raman	96		97	
ν_5	NO asymmetric stretch	infrared, Raman	1760		1762	1776.2
ν_6	N−N═O asymmetric bend	infrared, Raman		489	214	
ref			7	7	8	26

In some of our spectra, in addition to the absorptions of the cis form, weak features associated with the trans variety were also observed along with bands that could be attributed to the two remaining geometries of the dimer (*trans*- and *cis*-ONON).

It should be already noticed that NO behaves in a quite different way according to the nature (argon or nitrogen) of the matrix under study. Bands obtained in argon matrixes are wide and flat, while they become sharp with a well-defined structure in N_2 matrixes. As an example, in N_2 matrixes, the trans dimer is easily observed and the structure of each band is sharp and well-defined, although dimerization is far from complete. On the contrary, in argon matrixes, the proportion of NO monomers

* To whom correspondence should be sent. E-mail: krim@ccr.jussieu.fr.

S1089-5639(97)03327-6 CCC: $15.00
Published on Web 03/06/1998

TABLE 2: IR Absorption Frequencies and Assignments for ^{14}NO and ^{15}NO Trapped in Argon Matrix[a]

$^{14}NO-^{14}NO$	$^{14}NO-^{15}NO$	$^{15}NO-^{15}NO$	assignment
175.5	174.9	174.7	ν_3 *cis*-ON−NO
242.8	241.1	239.6	ν_6 *cis*-ON−NO
299.3	298.2	294.1	ν_2 *cis*-ON−NO
362.4	357.7	355.2	$2\nu_3$ or $\nu_6 + \nu_4$ *cis*-ON−NO
640.4	639.4	638.30	other form
746	740.3	735.6	N_2O_4 out-of-phase bend ν_{12}
903.6	898.1	892.8	other form or overtone
1256.6	1250.6	1244.6	N_2O_4 out-of-phase symmetric stretch ν_{11}
1688.6	1670.5	1660.4	ν_5 N═O a-stretch *cis*-ON−ON
1747.1	1721.2	1714.9	ν_5 a-stretch *trans*-ON−NO
1776.3	1757.6	1744.7	ν_5 a-stretch *cis*-ON−NO
1863.4	1849.7	1830.6	ν_1 s-stretch *cis*-ON−NO
1872.2	1839.2		NO−Ar complex
1879.70 = 1776.3 + 103.4	1860 = 1757.6 + 103.4	1847 = 1744.7 + 102.3	$\nu_5 + \nu_4$ *cis*-ON−NO
1969.70 = 1776.3 + 193.4	1948.6 = 1757.6 + 191	1934.1 = 1744.7 + 189.4	$\nu_5 + \nu_3$ *cis*-ON−NO
2026.2 = 1776.3 + 249.9	2005.3 = 1757.6 + 247.7	1990.9 = 1744.7 + 246.2	$\nu_5 + \nu_6$ *cis*-ON−NO
2106 = 1863.4 + 242.6	2091 = 1849.7 + 241.3	2070.1 = 1830.6 + 239.5	$\nu_1 + \nu_6$ *cis*-ON−NO
3531.4	3493.6	3469.4	$2\nu_5$ *cis*-ON−NO
3608.80	3580	3545.5	$\nu_1 + \nu_5$ *cis*-ON−NO
3713.5	3684.7	3648.3	$2\nu_1$ *cis*-ON−NO

[a] Wavenumbers are expressed in cm^{-1}. Monomer frequency: for ^{14}NO, 1874.53 cm^{-1}; for ^{15}NO, 1841.49 cm^{-1}.

is negligibly small (dimer formation is more important in argon matrix than in nitrogen matrix), and nevertheless, the trans dimer is hardly observed whereas the overtone and combination bands are much more easily detected. Therefore, it appears that studies in both argon and nitrogen matrixes will provide us with complementary information.

In the first part, the experimental conditions will be briefly described, and then the results obtained will be discussed and the derived harmonic force field will be presented.

2. Experiment

^{14}NO gas was provided by "L'Air Liquide" with a stated chemical purity of 99.9% and ^{15}NO gas by "Isotec" with an isotopical purity of 96% (4% ^{14}NO in ^{15}NO). Argon gas also from "L'Air Liquide" had a stated purity of 99.9995%, and it was used without any further purification.

The NO gas was first trapped in liquid nitrogen, then a small amount was allowed to evaporate, and the partial pressure so obtained was mixed with argon gas in order to obtain the desired concentration ratio NO/Ar. In the present study, ratios of 1/3000, 1/1000, 1/300, and 1/100 were used.

The mixture was then deposited onto a window cooled to 20 K in the case of argon matrix. The decrease of the pressure in the gas phase above the matrix was about 1 mbar/min. The gas was condensed onto the cold window at a rate of 10 mmol/h. Spectra were recorded every deposited 5 mmol. The total amount of the decrease of the pressure in the gas to be condensed was varied according to the intensity of the studied transitions, up to an upper limit of about 350 mbar corresponding to a total of 35 mmol deposited.

Very few NO_2 and N_2O impurities were detected from their absorptions located near 1284 and 2222 cm^{-1} for N_2O and 1623 cm^{-1} for NO_2.

Spectra were recorded using a FTIR Bruker spectrometer (IFS 120HR) at a resolution of 0.5 cm^{-1} in the 100−500 cm^{-1} range and 0.1 cm^{-1} in the 500−6000 cm^{-1} range. A bolometer detector was used for the low-frequency region, typically from 100 to 500 cm^{-1} and a MCT detector from 500 to 6000 cm^{-1}. No signal was observed beyond 3750 cm^{-1} under the present conditions. Each spectrum took about 20 mn to be recorded and was derived from the average of 200 scans.

For a given x mmol deposited ($5 \leq x \leq 35$), three kinds of spectra were recorded at a series of different temperatures:

spectra recorded at the temperature of deposition, 20 K, to check the evolution of each observed band;

spectra recorded after cooling the matrix down to the lowest limit of 7 K;

spectra recorded at 7 K, after previous heating of the matrix at several temperatures up to 35 K in order to vary and monitor the formation of dimers. In the following, all presented spectra are recorded at 7 K after an annealing of the matrix up to 30 K.

3. Vibrational Analysis

Spectra obtained from pure ^{14}NO or pure ^{15}NO exhibit roughly similar structure with the only difference that the frequencies of the dominant cis form are, for $O^{14}N^{14}NO$, a few wavenumbers higher than those of $O^{15}N^{15}NO$. A number of spectra were also taken with a mixture made of 50% ^{14}NO and 50% ^{15}NO. In these spectra each transition gives rise to a triplet structure whose components have relative intensities proportional to 1:2:1. This corresponds obviously to the respective contributions of the three forms, *cis*-$O^{14}N-^{14}NO$, *cis*-$O^{14}N-^{15}NO$, and *cis*-$O^{15}N-^{15}NO$. This peculiarity has been systematically used to ensure the frequency assignments. The observed frequencies for all of the studied isotopomers are listed in Table 2 as well as the proposed assignments.

A. Fundamental Modes. (a) The lowest frequency we were able to detect appears as a very weak signal located near 175 cm^{-1}. Figure 1 shows a band obtained for $O^{14}N-^{14}NO$. This frequency could be assigned as being the ν_3 N−N═O symmetric bending mode, which is in accordance with the similar attribution reported in most previous Raman studies (cf. Table 1). Durig et al.,[7] Smith et al.[16] and Nour et al.,[8] gave 176, 167, and 187 cm^{-1}, respectively, for this mode. In liquid or crystal phase as well as in CO_2 or CCl_4 matrixes, Laane et al.[22] listed different values, all of them near 170 cm^{-1} and attributed to ν_3.

(b) Two bands located near 243 and 300 cm^{-1} were observed. The intensity of each band grows up after annealing the matrix up to 30 K, while at the same time, the NO monomer band, located at 1874 cm^{-1} (see below, monomer region paragraph), decreases. These bands have the same intensity behavior as the *cis*-NO dimer ν_1 and ν_5 bands (see below) and could be attributed to ν_2 N−N stretching and ν_6 N−N═O asymmetric bending, the two left infrared active modes of *cis*-ON−NO.

For *cis*-$O^{14}N-^{14}NO$ and *cis*-$O^{15}N-^{15}NO$ pure dimers, a sharp peak was observed centered near 243 and 239 cm^{-1}, respec-

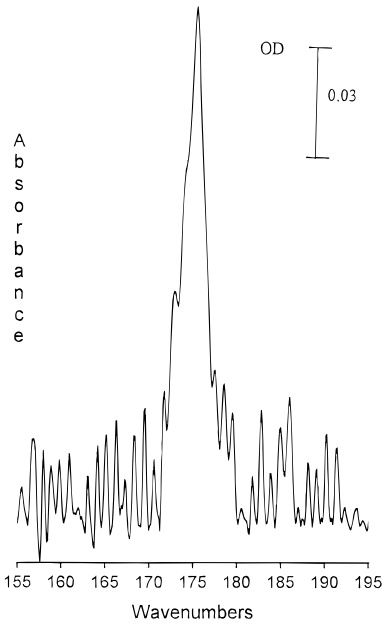

Figure 1. NO trapped in Ar matrix, the ν_3 symmetric ONN bending mode of *cis*-(^{14}NO)$_2$. Molar ratio NO/Ar is 1/300. 30 mmol deposited. (OD = optical density.) Integrated absorbance is equal to 0.07 cm^{-1}.

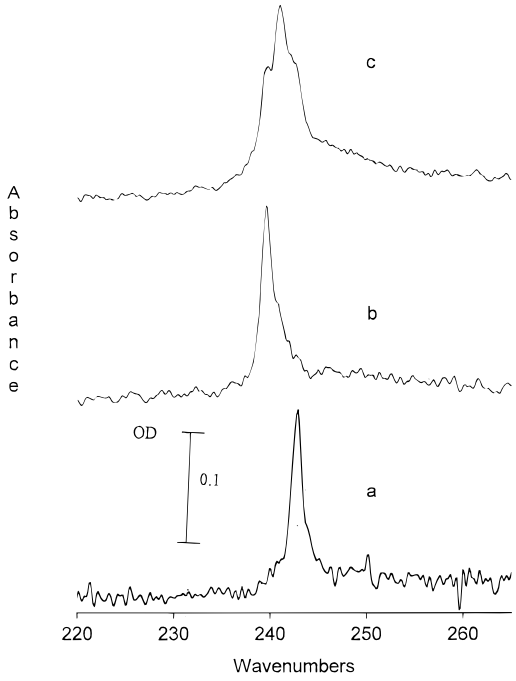

Figure 2. NO in Ar matrix, the ν_6 asymmetric ONN bending mode of *cis*-O═N−N═O. 30 mmol deposited. (a) ^{14}NO in Ar, 1/ 300; (b) ^{15}NO in Ar, 1/ 300; (c) ^{15}NO and ^{14}NO in Ar, 1/1/300. Integrated absorbance is equal to 0.3 cm^{-1} for spectrum a.

tively. Owing to the smallness of this shift, the spectrum obtained with the mixed species appears as a partially resolved wide envelope whose central peak falls near 241 cm^{-1} (cf. Figure 2).

Near 300 cm^{-1} lies a relatively wide band, consisting of three narrow peaks for both pure *cis*-O^{14}N−^{14}NO and *cis*-O^{15}N−^{15}NO. The peak structures are probably due to site effects. The frequency shift between the two pure dimer species is approximately 5 cm^{-1} so that the superimposition of the three triplets obtained for the mixed species results in a wide envelope showing a residual structure of doublets (cf. Figure 3).

These two bands, located near 243 and 300 cm^{-1}, are

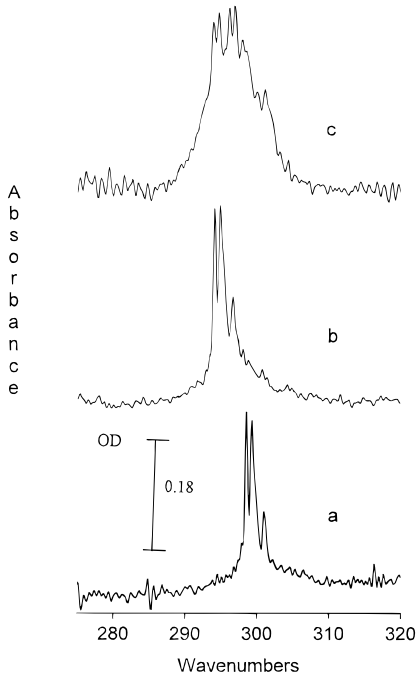

Figure 3. NO trapped in Ar matrix, the ν_2 N−N stretching mode of *cis*-O═N−N═O. 30 mmol deposited. (a) ^{14}NO in Ar, 1/ 300; (b) ^{15}NO in Ar, 1/300; (c) ^{15}NO and ^{14}NO in Ar, 1/1/300. Integrated absorbance is equal to 0.75 cm^{-1} for spectrum a.

separated by 57 cm^{-1}. In this spectral region Nour et al.[8] found two bands separated by 52 cm^{-1}, located at 214 and 266 cm^{-1}, respectively. They attributed the smaller frequency to the ν_6 N−N═O asymmetric bending mode and the larger one to the ν_2 N−N stretching mode. Laane et al.[22] gathered couples of frequencies for the ν_6 and ν_2 modes, obtained from various experimental methods (liquid, crystal phase, matrix isolation). All their values are located near 200 cm^{-1} for the ν_6 N−N═O asymmetric bending and 260 cm^{-1} for the ν_2 N−N stretching, and, in each case, these bands are separated by 60 cm^{-1}. In our far-infrared study these two bands are separated by 57 cm^{-1}. The band lying near 243 cm^{-1} could then be attributed to the ν_6 N−N═O asymmetric bending mode, which is supported by our force-field calculation (see Section 5). The band lying near 300 cm^{-1} could be attributed to the ν_2 N−N stretching mode. The systematic blue shift of 30 cm^{-1} between our results and those given by other authors from solid-phase observations[7,8] could be due to solid-state effects where the N−N stretching and the ONN bending of *cis*-ON−NO can be strongly coupled with neighboring dimers. Comparison between results obtained in solid phase and in argon matrix is presented below.

(c) The most intense bands are those due to the N═O asymmetric stretch ν_5 and the N═O symmetric stretch ν_1, which lie in the 1740−1780 and 1820−1870 cm^{-1} regions, respectively, and were previously extensively studied.[9−11] In the case of the ν_5 band, Figure 4 shows the large frequency shift from ^{14}NO to ^{15}NO (approximately 30 cm^{-1}). Accordingly the mixed species exhibits three widely separated structures corresponding to the three varieties of the *cis*-ONNO dimer. Each ν_5 isotopic band is composed of four extra peaks, probably owing to site effects. Moreover, for each kind of isotopic dimer, a wide and weak band red-shifted by 6 cm^{-1} from the ν_5 band is observed. This band is sensitive to the change of the isotopic composition of the NO. Therefore it seems clear that this feature originates from a NO dimer, but we are not able to identify it so far.

(d) The ν_5 intensities of the cis dimer are about 500 times larger than those of the trans dimer. Nevertheless, the ν_5 band

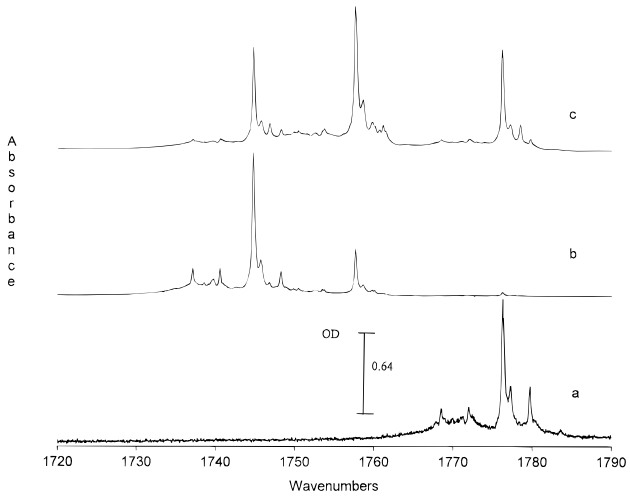

Figure 4. NO in Ar matrix, the ν_5 NO asymmetric stretching mode of *cis*-O═N−N═O. 5 mmol deposited. (a) ^{14}NO in Ar, 1/900; (b) ^{15}NO in Ar, 1/ 900; (c) ^{15}NO and ^{14}NO in Ar, 1/1/900. Integrated absorbance is equal to 1 cm^{-1} for spectrum a.

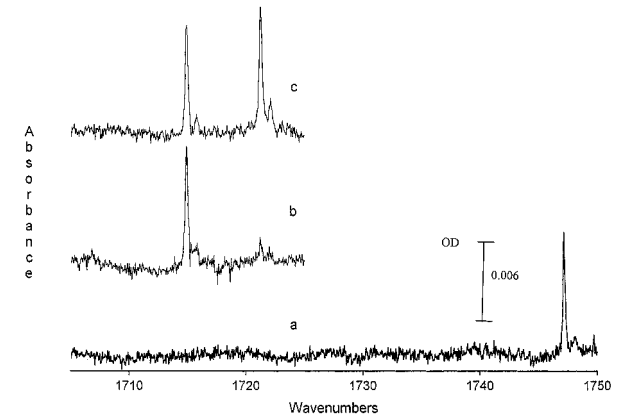

Figure 5. NO in Ar matrix, the ν_5 NO asymmetric stretching mode of *trans*-O═N−N═O. 30 mmol deposited. (a) ^{14}NO in Ar, 1/900; (b) ^{15}NO in Ar, 1/900; (c) ^{15}NO and ^{14}NO in Ar, 1/1/900.

of the latter species is observed around 1747.1 cm^{-1} for *trans*-O^{14}N^{14}NO, 1721.2 cm^{-1} for *trans*-O^{14}N^{15}NO, and 1714.9 cm^{-1} for *trans*-O^{15}N^{15}NO (cf. Figure 5). This band was previously observed near 1740 cm^{-1} by Fateley et al.[23] for the O^{14}N^{14}NO species in a CO_2 matrix and near 1759.57 cm^{-1} in a N_2 matrix by Legay et al.[24,25] The ν_5 N═O asymmetric stretch, for *trans*-ONNO, was also observed in N_2 matrix as an intense signal around 1760.03, 1742.01 and 1728.90 cm^{-1} for *trans*-O^{14}N^{14}-NO, *trans*-O^{14}N^{15}NO, and *trans*-O^{15}N^{15}NO, respectively.[21]

Figure 6 shows the spectral structure attributed to ν_1 N═O symmetric stretch of *cis*-ONNO. It is composed of a sharp and intense peak along with three weak extra peaks located around the main peak. These three peaks can be due to site effects.

B. Overtone and Combination Bands. The overtone and combination bands of ν_1 and ν_5 modes have also been observed in the spectral region beyong 3400 cm^{-1}. The $\nu_1 + \nu_5$ combination is observed in the 3540−3620 cm^{-1} range for each one of the *cis*-NO dimers. It was already observed by Canty et al.[26] in matrix and by Menoux et al. [13] and Hetzler et al.[27] in gas phase. In our spectra, each band consists of three peaks, due to site effects, as can be seen in Figure 7. The overtone frequencies $2\nu_5$ and $2\nu_1$ are observed in the 3460−3540 (Figure 8) and 3610−3720 cm^{-1} spectral intervals, respectively.

Two other combination bands are observed around 1980−2030 cm^{-1}, the $\nu_5 + \nu_6$ (see Figure 9) and around 2060−2110 cm^{-1}, the $\nu_1 + \nu_6$ band.

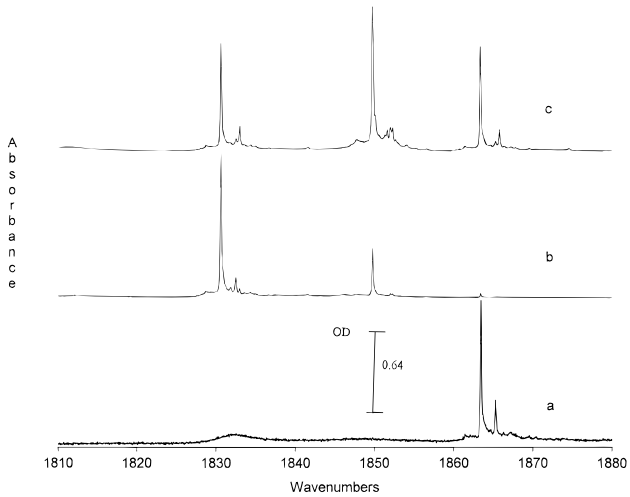

Figure 6. NO in Ar matrix, the ν_1 NO symmetric stretching mode of *cis*-O═N−N═O. 5 mmol deposited. (a) ^{14}NO in Ar, 1/900. (b) ^{15}NO in Ar, 1/900; (c) ^{15}NO and ^{14}NO in Ar, 1/1/900. Integrated absorbance is equal to 0.36 cm^{-1} for spectrum a.

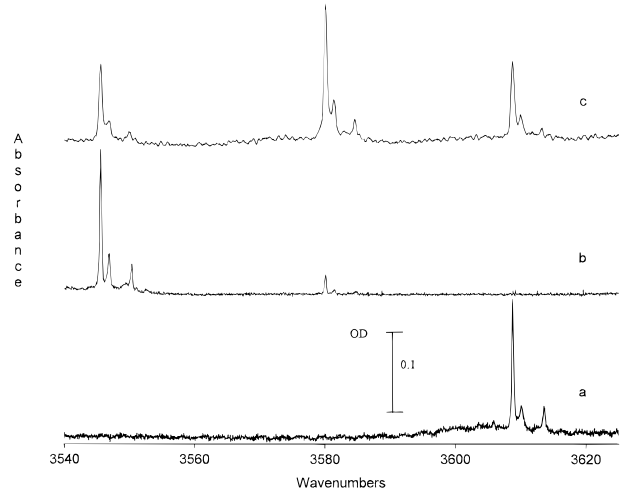

Figure 7. NO in Ar matrix, $\nu_1 + \nu_5$ combination band of *cis*-O═N−N═O. 30 mmol deposited. (a) ^{14}NO in Ar, 1/900; (b) ^{15}NO in Ar, 1/900; (c) ^{15}NO and ^{14}NO in Ar, 1/1/900. Integrated absorbance is equal to 0.032 cm^{-1} for spectrum a.

In the 1920−1980 cm^{-1} region, the $\nu_3 + \nu_5$ combination band is also observed. In the 1865−1880 cm^{-1} region another peak can be observed for each isotopomer at a frequency nearly equal to $\nu_5 + 103$ cm^{-1}. Therefore 103.4 cm^{-1} could be attributed to the ν_4 IR-inactive mode for the *cis*-O^{14}N−^{14}NO. The ν_4 frequency was also calculated for the two other isotopomers, and it was found to be 103.4 cm^{-1} for O^{14}N^{15}NO and 102.3 cm^{-1} for O^{15}N^{15}NO (Table 2). It should be noticed that the ν_4 frequency is determined at ±1 cm^{-1} for O^{15}N^{14}NO. Nour et al.[8] previously found the ν_4 mode near 97 cm^{-1}, which is in rather good agreement with the present measurement, the difference being less than 10%. Laane et al.[22] propose two values for the ν_4 mode obtained in crystal phase, 97 cm^{-1} in Raman detection and 96 cm^{-1} for infrared study.

In the far-infrared spectra a weak band is observed near 360 cm^{-1}. Its position and intensity depend on NO isotopic substitution and NO concentration. It could be attributed either to the $\nu_6 + \nu_4$ combination band or $2\nu_3$ overtone band.

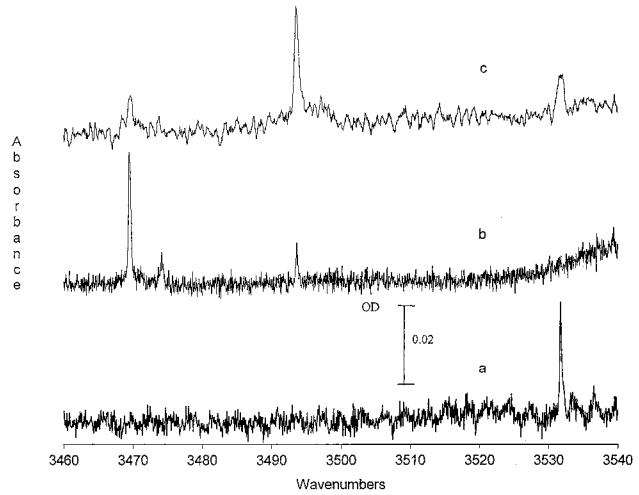

Figure 8. NO in Ar matrix, $2\nu_5$ overtone band of the NO asymmetric stretch of *cis*-O═N−N═O. 30 mmol deposited. (a) ^{14}NO in Ar, 1/900; (b) ^{15}NO in Ar; 1/900; (c) ^{15}NO and ^{14}NO in Ar, 1/1/900. Integrated absorbance is about 2.6×10^{-3} cm^{-1} for spectrum a.

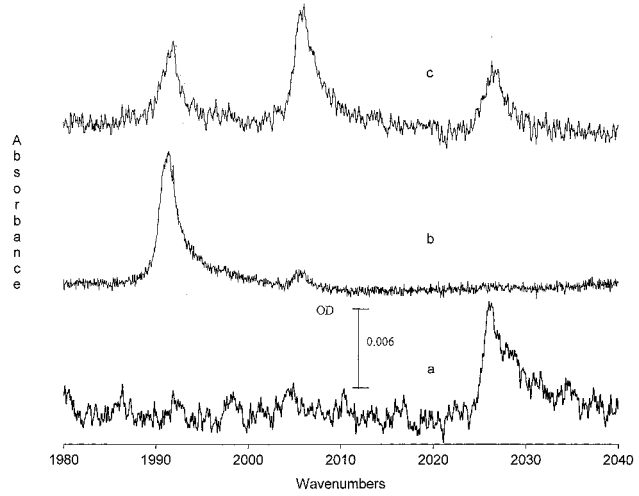

Figure 9. NO in Ar matrix, $\nu_5 + \nu_6$ combination band of *cis*-O═N−N═O. 30 mmol deposited. (a) ^{14}NO in Ar, 1/900; (b) ^{15}NO in Ar, 1/900; (c) ^{15}NO and ^{14}NO in Ar, 1/1/900.

Nevertheless, from Raman observation, Nour et al.[8] proposed 347 cm^{-1} for the $\nu_4 + \nu_6$ band and did not observe any overtone $2\nu_3$.

Among frequencies lower than 1700 cm^{-1}, some bands have an intensity that varies with concentration, pressure, isotopic composition of NO, and temperature of the matrix. These bands are located near 630, 730, 890, and 1240 cm^{-1}, respectively. These new-observed frequencies could be attributed to different modes of the trans dimer. In N_2 matrix these bands become much stronger. However, the bands near 730 and 1240 cm^{-1} could also be attributed to N_2O_4 out-of-phase bending ν_{12} and N_2O_4 out-of-phase symmetric stretch ν_{11},[22] respectively, so that an ambiguity subsists as to their definitive assignment.

In the 1660−1690 cm^{-1} region, another new band is observed (cf. Figure 10). It could characterize the ν_1 or ν_2 N═O stretch of a new geometry of *cis*-O═N−O═N. Its observed frequency, in the O^{14}NO^{14}N case, is equal to 1688.56 cm^{-1}, while the frequency predicted in refs 6 and 28 for the same isotopic species is 1690 cm^{-1}. Another frequency was predicted near 1778 cm^{-1},[6] which is unfortunately in the region of the ν_5 of the *cis*-O^{14}N−^{14}NO.

C. Monomer Region. ^{14}NO spectral signature presents two absorption bands; the first one consists of a sharp feature

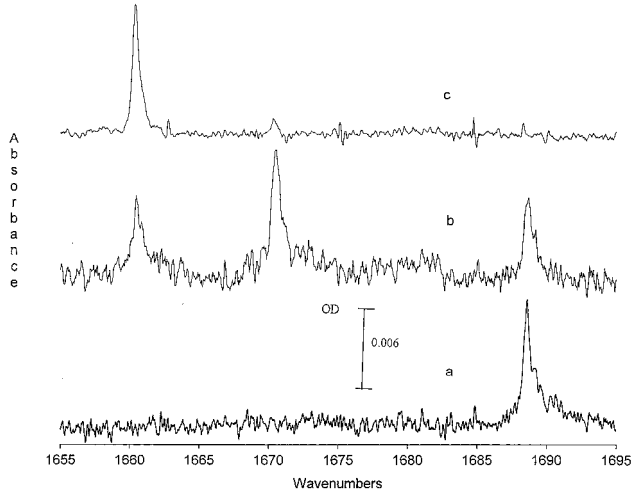

Figure 10. NO in Ar matrix, the ν_2 NO asymmetric stretching region of *cis*-ON−ON. 30 mmol deposited. (a) ^{14}NO in Ar, 1/900; (b) ^{15}NO in Ar, 1/900; (c) ^{15}NO and ^{14}NO in Ar, 1/1/900.

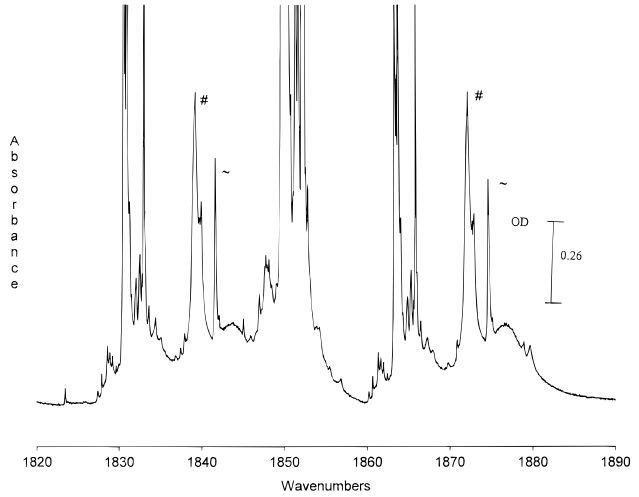

Figure 11. ^{15}NO and ^{14}NO in Ar, 1/1/900, monomer region. 30 mmol deposited. Peaks labeled ~ characterize the monomer. Peaks labeled # could be due to NO−Ar complex.

centered at 1874.5 cm^{-1}, and the second one is a much wider band centered at 1872.2 cm^{-1}. An example of these two features is presented in Figure 11. The second band could be due to the ^{14}NO−Ar complex. This is corroborated by observations in N_2 matrix, where only one monomeric band is observed around 1875 cm^{-1}. The same is observed in the case of ^{15}NO, where the sharp peak is centered at 1841.5 cm^{-1} and the wider one at 1839.2 cm^{-1}.

4. Discussion

A. Matrix Isolation and Solid Phase. The ν_1 band of the *cis*-ONNO isolated in argon matrix is located at 1863.4 and 1830.6 cm^{-1} for $(^{14}NO)_2$ and $(^{15}NO)_2$, respectively. These values become, in solid phase,[8] 1866 and 1832 cm^{-1}, respectively, while a red shift of 2.6 cm^{-1} is observed for $(^{14}NO)_2$ and 1.4 cm^{-1} for $(^{15}NO)_2$.

For the ν_5 band, a blue shift of 14.3 cm^{-1} is observed for $(^{14}NO)_2$ and 14.7 cm^{-1} for $(^{15}NO)_2$ (1776.3 and 1744.7 cm^{-1} in argon matrix, 1762 and 1730 cm^{-1} in solid state for all isotopomers). Therefore, one can notice that the N═O asymmetric stretching mode is more perturbed by the NO dimer environment than the N═O symmetric stretching mode.

TABLE 3: Relative Concentration of Dimer for ^{14}NO in Ar (NO/Ar Ratio Is 1/3000) and Absorption Intensities (Expressed in cm^{-1}) of ν_1 and ν_5 for *cis*-$O^{14}N^{14}NO$ and ^{14}NO at 7 K (5 mmol Deposited)

T (K)	I_{ν_1} (*cis*)	I_{ν_5} (*cis*)	(I_{ν_5}/I_{ν_1})	I_{NO}
7 K/20 K	0.085	0.238	2.80	0.338
7 K/25 K	0.097	0.275	2.83	0.252
7 K/35 K	0.106	0.299	2.82	0.196

In a same way, on the low-frequency side, the two bands located near 243 and 300 cm^{-1} separated by 57 cm^{-1} and attributed to the ν_6 and ν_2 modes, respectively, could be the same bands as those observed in the solid state by Durig et al.[7] and Nour et al.,[8] while a blue shift of 30 cm^{-1} is observed between our results and those obtained in the solid state.

In argon matrix, the ν_6 band of *cis*-ONNO is located near 242.8 and 239.6 cm^{-1} for $(^{14}NO)_2$, and $(^{15}NO)_2$, respectively. These values become, in solid phase, 214 and 209 cm^{-1}, respectively. A blue shift of 28.8 cm^{-1} is observed for $(^{14}NO)_2$ and of 30 cm^{-1} for $(^{15}NO)_2$.

The ν_2 band is located near 299.3 and 294.1 cm^{-1} for $(^{14}NO)_2$ and $(^{15}NO)_2$, respectively, in argon matrix. These band are red shifted in the solid state, by 33.3 and 33.1 cm^{-1} for $(^{14}NO)_2$ and $(^{15}NO)_2$, respectively.

The N−N stretching and the ONN asymmetric bending modes seem to be strongly perturbed by the NO environment in solid state, and this could explain the frequency differences of 12% for ν_2 and ν_6 between Nour et al.[8] and Durig et al.[7] on one hand and our results on the other hand.

The ν_3 band located near 174 cm^{-1} is close to the values given by other authors.[7,8,22] This mode seems to be unperturbed by the NO environment in the solid state.

Finally, one can notice that the ν_1 symmetric stretching mode is less perturbed by the environment in the solid state, than the ν_5 asymmetric stretching mode. In the same way, the ν_3 symmetric bending mode is less perturbed in the solid state than is the ν_6 asymmetric bending mode.

B. Band Intensities. The symmetric ν_1 and asymmetric ν_5 bands are characterized by well-defined spectral structures allowing precise intensity measurements. The order of magnitude of their intensity (integrated absorbance) ratio (I_{ν_5}/I_{ν_1}) is found to be 2.8. Table 3 presents the evolution of the intensity of these two bands as a function of the matrix temperature. It should be noticed that all spectra are recorded at $T = 7$ K, after an annealing of the matrix. When heating the matrix, an increase of the intensity of the dimer bands is observed whereas the intensity of the monomer band is decreased. The ratio of the absorption coefficient of the monomer to the absorption coefficient of the dimer can be derived. If $C_D(T)$ and $C_M(T)$ are the concentrations of the dimer and the monomer, respectively, while $I_D(T)$ and $I_M(T)$ are the absorption intensities of the dimer and the monomer, one can write, for two different temperatures T and T' of the matrix

$$I_M(T) = \alpha_M C_M(T) \quad \text{and} \quad I_D(T) = \alpha_D C_D(T) \tag{1}$$

$$I_M(T') = \alpha_M C_M(T') \quad \text{and} \quad I_D(T') = \alpha_D C_D(T') \tag{2}$$

where α_M and α_D are the absorption coefficients per unit concentration of the monomer and the dimer, respectively. It is, moreover, assumed that α_M and α_D are temperature-independent. For the lowest concentration (molar ratio NO/Ar is 1/3000), the absorption due to the monomer is low enough to allow a precise evaluation of $I_M(T)$ and $I_M(T')$. Therefore, assuming that there are only exchanges between monomeric and dimeric forms, one can write

$$C_M(T) - C_M(T') = -2[C_D(T) - C_D(T')] \tag{3}$$

The ratio α_M/α_D can then be expressed as

$$\frac{\alpha_M}{\alpha_D} = -0.5\,\frac{I_M(T) - I_M(T')}{I_D(T) - I_D(T')} \tag{4}$$

and can be calculated: it is the half of the slope of the curve $I_M = f(I_D)$; an example of such a plot is given in Figure 12. The values $\alpha_M/\alpha_D = 1.16$ and $\alpha_M/\alpha_D = 3.4$ were found for the asymmetric mode ν_5 and the symmetric mode ν_1, respectively. The asymmetric mode is thus about three times more absorbant than the symmetric one, which is in good agreement with the direct determination of the intensity ratio (I_{ν_5}/I_{ν_1}) equal to 2.8.

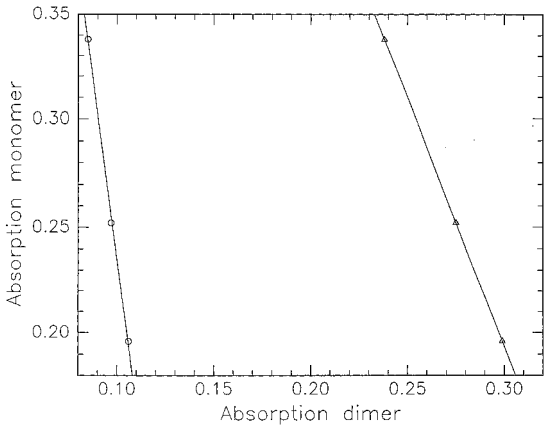

Figure 12. Temperature effect on the integrated absorbances of the NO band and the ν_5 and ν_1 bands of *cis*-ON−NO: ○, integred absorbance of ν_1 band; △, integred absorbance of ν_5 band.

TABLE 4: Relative Absorption Intensities of ν_1, ν_5 Overtone and Combination Bands for *cis*-$O^{14}N^{14}NO$

bands	intensity
ν_5	1
ν_1	0.357
$2\nu_5$	2.6×10^{-3}
$\nu_1 + \nu_5$	0.032
$2\nu_1$	10^{-3}

Table 4 gathers the intensities measured for the fundamentals ν_1 and ν_5 of *cis*-$O^{14}N^{14}NO$ along with those of the corresponding overtones and combination bands, $2\nu_1$, $2\nu_5$, and $\nu_1 + \nu_5$. It can be noticed that the ratio $(I_{2\nu_5}/I_{2\nu_1})$ is equal to 2.6, which is consistent with the value (I_{ν_5}/I_{ν_1}) determined above. The $\nu_1 + \nu_5$ combination band intensity is 30 times higher than those of the symmetric overtone band.

C. Anharmonicity Coefficients. From the knowledge of fundamental and overtone frequencies, anharmonicity coefficients can be evaluated. From a fundamental frequency ν_i and its overtone ν_{2i}, the anharmonicity coefficient x_{ii} is defined by[30]

$$2\nu_i - \nu_{2i} = 2x_{ii} \tag{5}$$

From two fundamental frequencies ν_i and ν_j and their combination frequency ν_{i+j}, the anharmonicity coefficient x_{ij} is defined by[30]

$$(\nu_i + \nu_j) - \nu_{i+j} = x_{ij} \tag{6}$$

We shall assume that anharmonicity coefficients x_{ii} and x_{ij} could be considered as independent of isotopic substitution;[30]

TABLE 5: Vibrational Anharmonicity Coefficients of NO Dimer (cm^{-1})

anharmonicity coefficients	$^{14}NO-^{14}NO$	$^{14}NO-^{15}NO$	$^{15}NO-^{15}NO$
x_{11}	6.62	7.39	6.45
x_{15}	30.81	27.36	29.79
x_{16}	0.2	−0.2	0.1
x_{53}	−17.9	−16.1	−14.6
x_{55}	10.5	10.8	10
x_{56}	−7.1	−6.6	−6.5

therefore, the isotopic shifts must verify the following equations

$$\nu_{2i} - \nu^*_{2i} = 2(\nu_i - \nu^*_i) \quad (7)$$

$$\nu_{i+j} - \nu^*_{i+j} = (\nu_i - \nu^*_i) + (\nu_j - \nu^*_j) \quad (8)$$

where the ν^* denote the frequencies of the isotopic dimers. Therefore, eqs 7 and 8 should be verified for each couple of dimers. From the values of the ν_1, ν_5, $2\nu_1$, $2\nu_5$, and $\nu_1 + \nu_5$ frequencies of each one of the isotopic dimers, the anharmonicity coefficients x_{11}, x_{55}, and x_{15} have been calculated (cf. Table 5).

The values of the anharmonicity coefficients were found to be nearly identical for $(^{14}NO)_2$ and $(^{15}NO)_2$, the deviation never exceeding 3%. The deviation becomes much larger, about 10%, for the mixed species $O^{14}N-^{15}NO$.

From combination bands between the N═O streching and the ONN bending modes, similar calculation was performed for obtaining the x_{56}, x_{53}, and x_{16} anharmonicity coefficients from the values of the $\nu_5 + \nu_6$, $\nu_3 + \nu_5$, and $\nu_1 + \nu_6$. Equation 8 was also found to be verified to good precision (cf. Table 5). The values of the x_{56} and x_{53} coefficients are found to be negative for the three isotopic species, while the x_{16} can be ranked to 0 cm^{-1}.

The ν_6 band intensity of *cis*-ONNO is about 10 times stronger than the one of ν_3 band. Therefore, the band located near 360 cm^{-1} is probably the combination band $\nu_4 + \nu_6$ and not the overtone $2\nu_3$. From the knowledge of the ν_6 and $\nu_4 + \nu_6$ bands for each isotopomer, a calculation was performed for obtaining the ν_4 frequency. Values equal to 119.6, 116.6, and 115.6 cm^{-1} were found for $O^{14}N^{14}NO$, $O^{14}N^{15}NO$, and $O^{15}N^{15}NO$, respectively. These calculated values of the ν_4 mode are different from those obtained from the $\nu_4 + \nu_5$ combination bands. This deviation around 10% is probably due to the difference between x_{45} and x_{46} anharmonicity coefficients.

5. Force Constant Calculations

Among the four possible geometries of $(NO)_2$,[6] the most stable species is known to be the *cis*-ON−NO. In the ground state, its geometry is well-established, and various sets of structural parameters have already been proposed,[8,31] all of them in relative good agreement. The most recent set is given in ref 29 where the bond lengths for N−N and O═N are given to be 2.278 and 1.155 Å, respectively, while the N−N═O angle is 97.8°.

To determine a complete set of force constants for *cis*-ON−NO and to check the consistency of our assignments, a harmonic force-field calculation was carried out, using all observed frequencies for the three isotopic species.

The internal coordinates used in the calculation are the N−N bond length, R, the N═O lengths, r_1 and r_2, the bending angles, α_1 and α_2, and the torsion angle, τ.[8,31,32]

The force constants have been determined for two different sets of structural parameters at equilibrium. The first one is the set proposed by McKellar et al.,[31] where $r_{NO} = 1.1515$ Å, $R_{NN} = 2.263$ Å, and $\alpha_{NNO} = 97.17°$. The second one is the one determined by Western et al.[33] and previously used by Nour et al.[8] The parameters of this set are $r_{NO} = 1.15$ Å, $R_{NN} = 2.33$ Å, and $\alpha_{NNO} = 95°$.

TABLE 6: Force Constants for *cis*-ON−NO[a]

		this work		calc M	calc N
constant	description	set 1	set 2	ref 29	ref 8
f_r	N−O stretch	14.677	14.639	14.684	14.487
f_R	N−N stretch	0.390	0.390	0.308	0.323
f_α	ONN bend	0.415	0.423	0.782	0.340
f_τ	torsion	0.029	0.03	0.036	0.02
$f_{r\alpha}$	N−O, ONN[b]	0.115	0.115		0.111
$f_{r\alpha'}$	N−N, ONN[c]	−0.008	−0.008		0.0
$f_{R\alpha}$	N−N, ONN	0.125	0.126	0.269	0.149
$f_{\alpha\alpha}$	ONN, ONN	0.169	0.166		0.171
f_{rr}	N−O, N−O	0.736	0.700	0.783	0.778
f_{Rr}	N−N, N−O	0.882	0.878	0.637	−0.079

[a] Calc M: McKellar et al.[29] Calc N: Nour et al.[7] Set 1: $r_{NO} = 1.1515$ Å, $r_{NN} = 2.263$ Å, and $\alpha_{NNO} = 97.17°$. Set 2: $r_{NO} = 1.15$ Å, $r_{NN} = 2.33$ Å, and $\alpha_{NNO} = 95°$. [b] $f_{r\alpha}$: interaction of the N−O stretching with the nearest bending angle NNO. [c] $f_{r\alpha'}$: interaction of the N−O stretching with the more distant bending angle NNO. The units are mdyn/Å for f_r, f_R, f_{rr}, and f_{Rr}, mdyn/rad for $f_{r\alpha}$ and $f_{R\alpha}$, and mdyn Å/rad^2 for f_α, f_τ, and $f_{\alpha\alpha}$.

TABLE 7: Potential Energy Distribution[a] for *cis*-ON−NO

frequency (cm^{-1})	f_r	f_R	f_α	f_τ	modes
1863.4	99.7	0	0.3	0	ν_1
1776.3	82.4	0	17.6	0	ν_5
299.3	0.3	52.4	47.3	0	ν_2
242.9	0	0	100	0	ν_6
175.4	0.5	88.5	11	0	ν_3
103.4	0	0	0	100	ν_4

[a] Normalized to a total of 100 for the diagonal force constant distributions within each vibration.

The 10 force constants determined in the present study are displayed in Table 6 and compared to those derived by Nour et al.[8] along with those obtained more recently by McKellar et al.[31] The force constants we obtained with the two above-mentioned sets are almost identical. The deviations between the two calculations never reach 5% and are very often much smaller. Our values seem to be in better agreement with Nour et al.[8] than they are with McKellar et al.,[31] except for the interaction constant f_{Rr}, which is closer to the result of McKellar. The important disagreement found with McKellar's values is probably due to his neglect of the off-diagonal force constants $f_{r\alpha}$, $f_{r\alpha'}$, and $f_{\alpha\alpha'}$ whose order of magnitude turns out to be far from negligible.

Observed and calculated frequencies for the three isotopic species and the two sets of structural parameters are presented in Table 7. The experimental frequency taken for the ν_4 (around 103 cm^{-1}) is obtained from the $\nu_4 + \nu_5$ frequency (cf. Table 2).

For each isotopic variety, the potential energy distribution was also calculated. Table 7 summarizes the results for the different vibrations of *cis*-$(N^{14}O)_2$. The potential energy distribution of each vibration[8] shows that there are two kinds of modes: pure modes and coupled modes. It can be noticed that the four bands located at 1863.4, 1776.3, 242.9, and 103 cm^{-1} present the modes that are mainly uncoupled or pure modes. In particular, the frequency at 242.9 cm^{-1}, corresponding to a pure ONN bending, could be attributed to the ν_6 mode. Similarly, the 299.3 and 175.4 cm^{-1} frequencies, involving mainly the N−N stretching, could be attributed to ν_2 and ν_3

modes, respectively. However, the N−N stretching and NNO bending are strongly coupled.

The potential energy distribution appears very insensitive to isotopic substitution for all modes except for ν_1. For this mode, the energy located on the NNO bending stands around 0.3% for both (^{14}NO) and (^{15}NO), while it reaches 1% for the mixed O^{14}N−^{15}NO. This evolution, even though the relative energy remains weak, represents an increase by a factor of 3. It shows also that, for the ν_1 mode, the NNO bending is three times more excited in the case of the mixed dimer than it is for pure dimers. This increase would probably facilitate the intramolecular vibrational energy relaxation and therefore have an effect on the lifetime of the ν_1 level. McKellar et al.[31] measured vibrational predissociation widths for symmetric and mixed isotopes. They found 0.014 cm^{-1} for the mixed species and around 0.005 cm^{-1} for the pure ones, which means that the lifetime is three times larger for the pure isotopes than it is for the mixed one. A similar argument can be put forward for explaining the strong difference observed between ν_1 and ν_5 lifetimes (ref 10 and references cited therein). M. P. Casassa[34] observed that the ν_1 and the ν_5 modes lead to dissociation with very different rates. He measured (39 ± 8) and (880 ± 260) ps lifetimes for ν_5 and ν_1, respectively. The ν_5 has a faster channel of dissociation, probably due to the coupling between the O═N asymmetric stretching and the ONN bending.

6. Conclusion

Fundamental and combination bands of ^{14}NO−^{14}NO and its isotopomers, ^{14}NO−^{15}NO and ^{15}NO−^{15}NO, isolated in argon matrix have been observed in the far-, mid-, and near-infrared regions by Fourier transform spectroscopy. This study allowed us to identify and measure the frequencies of the five IR-active modes ν_1, ν_2, ν_3, ν_5, and ν_6 of *cis*-ON−NO. From the combination band $\nu_4 + \nu_5$, the frequency of the sixth mode, which is Raman active only, was also determined.

Another geometry of the NO dimer was suggested from the presence of a band observed at 1689 cm^{-1} that could not assign to (^{14}NO)$_2$. The *trans*-ON−NO was also observed in argon matrix, but its signature remains much weaker than it is in nitrogen matrix.

Our results seem to mainly agree with the observations of Nour et al.[8] and Durig et al.[7] Nevertheless, for several frequencies some shifts remain between our obtained values and those given by these authors.

The two ν_1 and ν_5 modes of *cis*-ONNO were already well-known. But one can notice that, in the solid state, the ν_1 band is 2.6 cm^{-1} blue-shifted (1866 cm^{-1} [7,8]) with respect to our results in argon matrix (1863.4 cm^{-1}). In the same way, the ν_5 band is 14.3 cm^{-1} red-shifted (1776.3 cm^{-1} in argon matrix and 1762 cm^{-1} in solid phase[8]). These random shifts are probably due to solid-state effects. Nevertheless, high-frequency vibrations of NO dimer seem to be less perturbed in the solid state than low-frequency ones such as ν_2 or ν_6 modes, where the calculated shifts are about 30 cm^{-1}.

The force-field calculation provided additional information about the mode assignment and pointed out that the ν_2 mode that is commonly considered as a pure N−N stretching involves, in fact, both stretching and bending movements. In the same way, the NO symmetric stretching vibration ν_1 is found to be a pure mode, while the NO asymmetric stretching mode ν_5 is coupled to the ONN bending. The ν_5 has a faster channel of dissociation, probably due to the coupling between the O═N asymmetric stretching and the ONN bending.

Acknowledgment. The authors like to thank Dr. L. Manceron and Prof. J. P. Perchard for helpful discussions, and also Mrs D. Carrère for her help during the experiments.

References and Notes

(1) Dinerman, C.; Ewing, G. E. *J. Chem. Phys*. **1970**, *53*, 626.
(2) Matsumoto, Y.; Ohshima, Y.; Takami, M. *J. Chem. Phys*. **1990**, *92*, 937.
(3) Hawkins, M.; Downs, A. J. *J. Phys. Chem.* **1984**, *88*, 1527.
(4) Sodeau, J. R.; Withnall, R. *J. Phys. Chem.* **1985**, *89*, 4484.
(5) Davis, S. R.; Andrews, L.; Trindle, C. O. *J. Chem. Phys*. **1987**, *86*, 6027.
(6) Mélen, F.; Herman, M. *J. Phys. Chem. Ref. Data* **1992**, *21*, 831.
(7) Durig, J. R.; Griffin, M. G. *J. Raman. Spectrosc*. **1976**, *5*, 273.
(8) Nour, E. M.; Chen, L. H.; Strube, M. M.; Laane, J. *J. Phys. Chem.* **1984**, *88*, 756.
(9) Howard, B. J.; McKellar, A. R. W. *Mol. Phys*. **1993**, *78*, 55.
(10) Dkhissi, A.; Soulard, P.; Perrin, A.; Lacome, N. *J. Mol. Spectrosc*. **1997**, *183*, 12.
(11) Watson, J. K. G.; McKellar, A. R. W. *Can. J. Phys.* **1997**, *75*, 181.
(12) Kometer, R.; Legay, F.; Legay-Sommaire, N.; Schwentner, N. *J. Chem. Phys*. **1994**, *100*, 8737.
(13) Menoux, V.; Le Doucen, R.; Haeusler, C.; Deroche, J. C. *Can. J. Phys.* **1984**, *62*, 322.
(14) Brechignac, Ph.; De Benedictis, S.; Halberstadt, N.; Whitaker, B. J.; Avrillier, S. *J. Chem. Phys*. **1985**, *83*, 2064.
(15) Fischer, I.; Strobel, A.; Staecker, J.; Niedner-Schatteburg, G.; Müller-Dethlefs, K.; Bondybey, V. E. *J. Chem. Phys*. **1992**, *96*, 7171.
(16) Smith, A. L.; Keller, W. E.; Johnston, H. L. *J. Chem. Phys*. **1951**, *19*, 189.
(17) Anderson, A.; Lassier-Govers, B. *Chem. Phys. Lett*. **1977**, *50*, 124.
(18) Tachibana, A.; Suzuki, T.; Yamato, M.; Yamabe, T. *J. Mol. Struct*. **1990**, *231*, 291.
(19) Stirling, A.; Papai, I.; Mink, J.; Salahub, D. R. *J. Chem. Phys*. **1994**, *100*, 2910.
(20) Guillory, W. A.; Hunter, C. E. *J. Chem. Phys*. **1969**, *50*, 3516.
(21) Krim, L. To be published.
(22) Laane, J.; Ohlsen, J. R. *Prog. Inorg. Chem*. **1980**, *27*, 465.
(23) Fateley, W. G.; Bent, H. A.; Crawford, B. *J. Chem. Phys*. **1959**, *31*, 204.
(24) Legay, F.; Legay-Sommaire, N. *Chem. Phys. Lett*. **1993**, *211*, 516.
(25) Legay, F.; Legay-Sommaire, N. *J. Chem. Phys*. **1995**, *102*, 7798.
(26) Canty, J. F.; Stone, E. G.; Bach, S. B. H.; Ball, D. W. *Chem. Phys. Lett*. **1997**, *216*, 81.
(27) Hetzler, J. R.; Casassa, M. P.; King, D. S. *J. Phys. Chem.* **1991**, *95*, 8086.
(28) Ohlsen, J. R.; Laane, J. *J. Am. Chem. Soc*. **1978**, *100*, 6948.
(29) Kukolich, S. G.; Sickafoose, S. M. *Mol. Phys*. **1996**, *89*, 1659.
(30) Darling, B. T.; Dennison, D. N. *Phys. Rev*. **1940**, *57*, 128.
(31) McKellar, A. R. W.; Watson, J. K. G.; Howard, B. *J. Mol. Phys*. **1995**, *86*, 273.
(32) Levin, I. W.; Pearce, R. A. R. *Vib. Spectra* Struct. **1975**, *4*, 102.
(33) Western, C. M.; Langridge-Smith, P. R. R.; Howard, B. J.; Novick, S. E. *Mol. Phys*. **1981**, *44*, 145.
(34) Casassa, M. P. *Chem. Rev*. **1988**, *88*, 815.